

Directional O...F halogen bonds

Christian Jelsch* and Benoît Guillot

CRM2, UNR CNRS 7036, Institut Jean Barriol, Université de Lorraine, Vandoeuvre les Nancy CEDEX, France.

*Correspondence e-mail: christian.jelsch@univ-lorraine.fr

Received 14 March 2017

Accepted 23 March 2017

Keywords: halogen bonding; theoretical charge density.

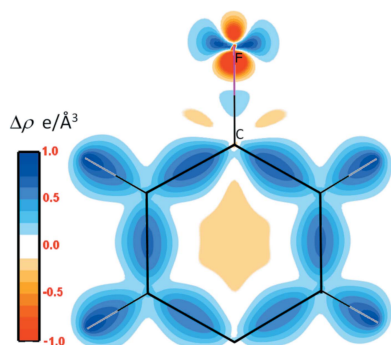
The study by Sirohiwal *et al.* (2017) analyzes the crystal structure and theoretical charge density of two organic compounds that display exceptionally short O...F halogen bonds. Compound A1 was selected from the Cambridge Structural Database while compound A2 was synthesized from the laboratory. A variety of state-of-the-art complementary tools for charge density analysis were applied.

Intermolecular contacts of the type $X \cdots O/N$ ($X = Cl, Br, I$) can be attractive and directional due to the anisotropic distribution of electron density on the halogen (Politzer *et al.*, 2007). Such non-covalent interactions are termed halogen bonding, where the halogen atoms function as electrophilic species. The deformation electron density of halogen atoms shows an accumulation of electrons in a crown perpendicular to the C—X bond where the three electron lone pairs are located and a depletion of electron density (σ -hole) on an extension of the C—X covalent bond (Fig. 1). The F atom is however different to the Cl, Br and I atoms as it is more electronegative and its σ -hole is much smaller. In the CSD-based study by Lommerse *et al.* (1996), it was even claimed that F...O/N halogen bonding does not occur at all. The F atom does however display a σ -hole, as found in a new deformation electron density by Sirohiwal *et al.* (2017). Another example of halogen bonding and evidence of a σ -hole for fluorine occurred in the experimental charge density of a highly fluorinated compound by Pavan *et al.* (2013) for which intermolecular F...F and F...S donor–acceptor contacts occur.

The fingerprint plots of molecular interactions on the Hirshfeld surfaces (McKinnon *et al.*, 2007) show that the O...F interactions account for 17.1% and 1.6% of the Hirshfeld surface in compounds A1 [1-(3-nitrophenyl)-2,2,2-trifluoroethanone] and A2 [(*E*)-4-(4-fluorophenyl) diazenyl]phenol], respectively. Analysis of the enrichment of crystal contacts highlights which types of interactions are over- or under-represented with respect to the chemical content on the Hirshfeld surface (Jelsch *et al.*, 2015). The crystal packings of compounds A1 and A2 are indeed peculiar. The O...F interactions are enriched at ratios of 1.2 and 3.0, respectively, which is unusual as halogen...oxygen contacts are generally found to be impoverished, while O...H and F...H contacts are more favored (Jelsch *et al.*, 2015).

Halogen bonding comprehensively covers a vast class of noncovalent interactions whose strength can vary in the range 10–200 kJ mol⁻¹ (Metrangolo *et al.*, 2008). Compound A1 contains a CF₃ moiety forming two interaction motifs (I) and (II), while compound A2 has an aromatic ring with one fluorine substitution corresponding to a third motif (III). In addition to stereochemical considerations, various approaches based on electronic distributions were applied to characterize and compare the strengths of the three O...F motifs: Quantum Theory of Atoms in Molecules, non-covalent interactions and electron delocalization index.

Pair-energy decomposition analysis, as implemented in the PIXEL method (Gavezzoti, 2011), gives access to the global intermolecular energy decomposition in terms of electrostatic, polarization, repulsion and dispersive contributions. The energetic analysis of the three dimers motifs with short O...F contacts shows that molecule A1, motif (II), which has a much longer F...O distance 3.146 Å (*versus* 2.871 and 2.709 Å), is the only one with significantly negative Coulomb and total energy. On the other hand, the Espinosa–Molins–Lecomte (EML) relationship (Espinosa & Molins, 2000) suggests conversely that the short F...O motifs have the strongest dissociation energy (D_{ev}). It has to be recalled here that the EML estimation of D_{ev} was designed only for X—H...O hydrogen bonds and may lead to unreliable results if extended to other systems (Spackman, 2015).



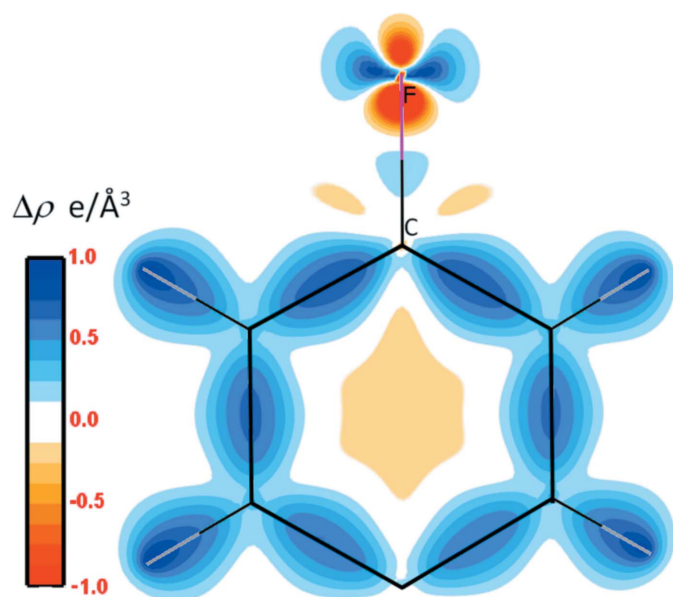


Figure 1
Contour plot of the deformation electron density of the C_6H_5F group.

The PIXEL analysis also provided an insight into the significant role of polarization on the stability of the three motifs. Hence, studying the distributed atomic polarizabilities appears to make sense here. Distributed atomic polarizability analysis was performed with the software *PolaBer* (Krawczuk *et al.*, 2014). The polarizability ellipsoids are indeed very elongated along the C–F direction for the F atoms (when bound to Csp^2 or Csp^3 atoms), which renders repulsive electrostatic contacts between two electronegative species in halogen-bonding geometry (C–F \cdots O not far from 180°) less unfavorable. The two short F \cdots O contacts [motifs (I) and (III)] indeed conform to that geometry. The polarizability tensors were obtained for dimers representative of the studied F \cdots O motifs and for isolated molecules *in vacuo*. This allowed

the authors to compare the representation quadrics of atomic polarizabilities in the two situations, and to show their evolution upon dimer formation. Notably it has been shown that the formation of the O \cdots F contact results in an increased polarizability of F atoms in the O \cdots F direction. In motifs (I) and (III), where the C–F \cdots O angle is close to 180° , it led to even more prolate ellipsoids. The ellipsoid was rendered more oblate in the case of motif (II) which is at a longer contact distance and where the C–F \cdots O angle of 101° is close to a right angle. The numerous charge density insights developed in the article are a good example in the field of crystal engineering of fine characterization of interatomic interactions. Finally, it has to be pointed out that in the case of motif (III), the O \cdots F short contact is supplemented by a weak O–H \cdots F hydrogen bond which is electrostatically attractive, as confirmed in the plot of electrostatic potential on the molecular surface. Interestingly, the optimized geometry of the dimer *in vacuo* did not contain the F \cdots O contact any longer.

References

- Gavezzotti, A. (2011). *New J. Chem.* **35**, 1360–1368.
 Jelsch, C., Soudani, S. & Ben Nasr, C. (2015). *IUCrJ.* **2**, 327–340.
 McKinnon, J. J., Jayatilaka, D. & Spackman, M. A. (2007). *Chem. Commun.* pp. 3814–3816.
 Espinosa, E. & Molins, E. (2000). *J. Chem. Phys.* **113**, 5686–5694.
 Krawczuk, A., Perez, D. & Macchi, P. (2014). *J. Appl. Cryst.* **47**, 1452–1458.
 Lommerse, J. P. M., Stone, A. J., Taylor, R. & Allen, F. H. (1996). *J. Am. Chem. Soc.* **118**, 3108–3116.
 Metrangolo, P., Meyer, F., Pilati, T., Resnati, G. & Terraneo, G. (2008). *Angew. Chem. Int. Ed.* **47**, 6114–6127.
 Pavan, M. S., Prasad, K. D. & Row, T. N. G. (2013). *Chem. Commun.* **49**, 7558–7560.
 Politzer, P., Lane, P., Concha, M. C., Ma, Y. & Murray, J. S. (2007). *J. Mol. Model.* **13**, 305–311.
 Sirohiwal, A., Hathwar, V. R., Dey, D., Roshni, R. & Chopra, D. (2017). *Acta Cryst.* **B73**, 140–152.
 Spackman, M. A. (2015). *Cryst. Growth Des.* **15**, 5624–5628.